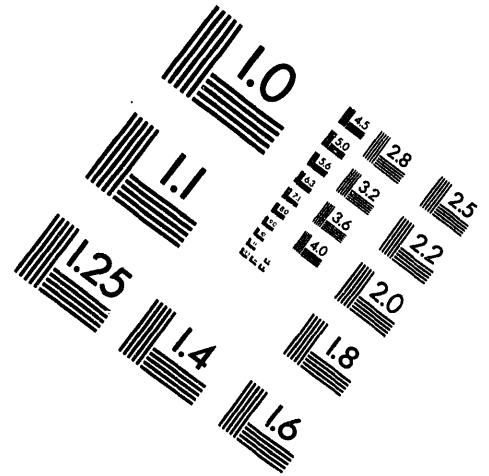
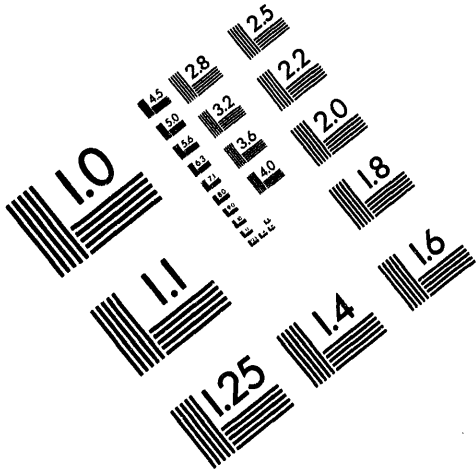




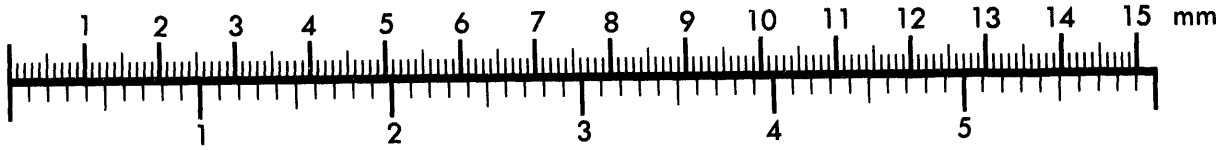
AIM

Association for Information and Image Management

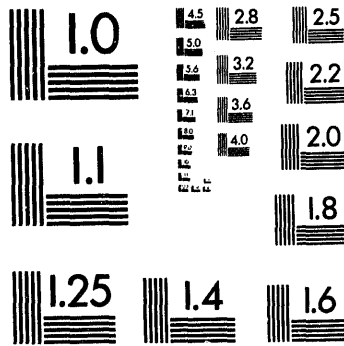
1100 Wayne Avenue, Suite 1100
Silver Spring, Maryland 20910
301/587-8202



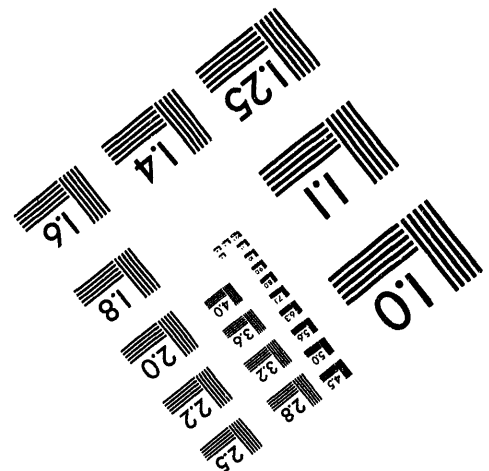
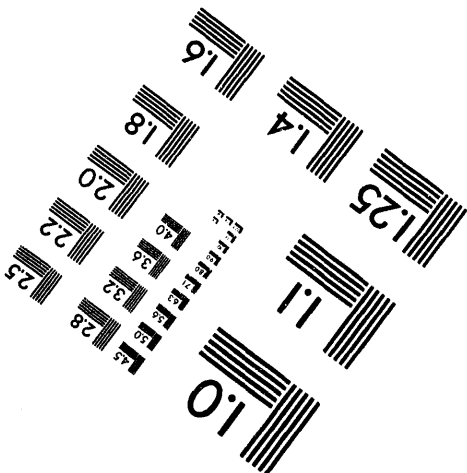
Centimeter



Inches



MANUFACTURED TO AIM STANDARDS
BY APPLIED IMAGE, INC.



1 of 1

DISCLAIMER

This report was prepared as an account of work sponsored by an agency of the United States Government. Neither the United States Government nor any agency thereof, nor any of their employees, makes any warranty, express or implied, or assumes any legal liability or responsibility for the accuracy, completeness, or usefulness of any information, apparatus, product, or process disclosed, or represents that its use would not infringe privately owned rights. Reference herein to any specific commercial product, process, or service by trade name, trademark, manufacturer, or otherwise does not necessarily constitute or imply its endorsement, recommendation, or favoring by the United States Government or any agency thereof. The views and opinions of authors expressed herein do not necessarily state or reflect those of the United States Government or any agency thereof.

Title:

EVALUATION OF SUPERCONDUCTING QUANTUM INTERFERENCE DEVICES INTERFACED WITH DIGITAL SIGNAL PROCESSING ELECTRONICS FOR BIOMAGNETIC APPLICATIONS

Author(s):

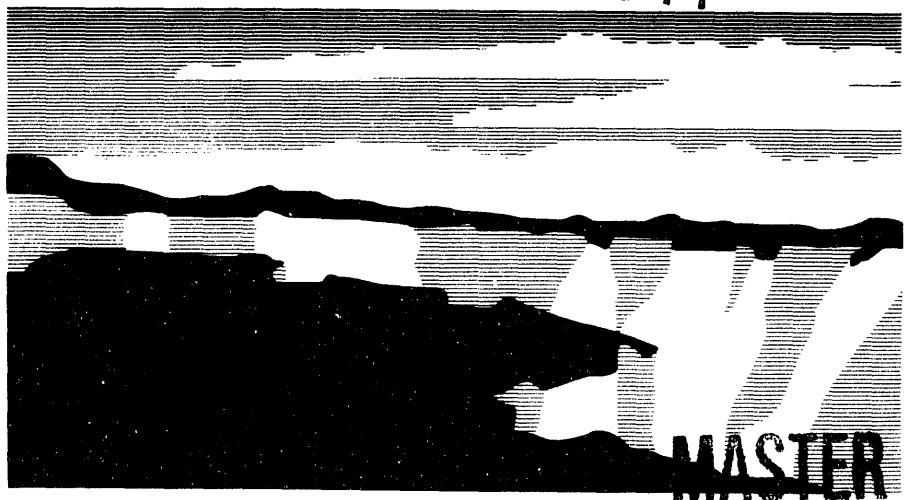
Pang Jen Kung
Edward R. Flynn
Roger R. Bracht
Paul S. Lewis

Submitted to:

The 5th International Conference on Signal Processing Applications and Technology
Dallas, Texas
October 18-21, 1994

CONFERENCE
OCT 18-21 1994
OSTI

Los Alamos
NATIONAL LABORATORY



MASTER

Los Alamos National Laboratory, an affirmative action/equal opportunity employer, is operated by the University of California for the U.S. Department of Energy under contract W-7405-ENG-36. By acceptance of this article, the publisher recognizes that the U.S. Government retains a nonexclusive, royalty-free license to publish or reproduce the published form of this contribution, or to allow others to do so, for U.S. Government purposes. The Los Alamos National Laboratory requests that the publisher identify this article as work performed under the auspices of the U.S. Department of Energy.

ds Form No. 836 R5
ST 2629 10/91

REPRODUCTION OF THIS DOCUMENT IS UNLIMITED

Evaluation of Superconducting Quantum Interference Devices Interfaced with Digital Signal Processing Electronics for Biomagnetic Applications

Pang-Jen Kung,¹ Edward R. Flynn,¹ Roger R. Bracht,² and Paul S. Lewis²

¹*Biophysics Group P-6, MS M715*

²*Systems and Robotics Group ESA-6, MS J580*

Los Alamos National Laboratory

Los Alamos, NM 87545

Tel: (505) 665-3057; Fax: (505) 665-4507

E-mail: kung@lawyer.lanl.gov

Abstract -- The performance of a dc-SQUID magnetometer driven by both analog electronics and digital signal processors are investigated and compared for biomagnetic applications. Low-noise ($< 5 \mu\Phi_0/\sqrt{\text{Hz}}$ at 1 Hz) dc-SQUIDs were fabricated by Conductus, Inc. using the all-refractory Nb/Al/Al₂O₃/Nb process on silicon substrates with on-chip modulation coils and integral washer damping resistors. A second-order gradiometer was magnetically coupled to the input coil of the SQUID to maximize the detected signal strength. The readout of this SQUID gradiometer was achieved using a conventional flux-locked loop (FLL) circuit to provide a linearized voltage output that was proportional to the flux applied to the SQUID. A shielded cylinder was constructed to house the magnetometer to reduce ambient field noise. To realize the digital feedback loop, the analog FLL is replaced except for the preamplifier by a digital signal processing board with dual 16-bit A/D and D/A converters. This approach shows several advantages over the analog scheme including operational flexibility, cost reduction, and possibly, the enhancement of dynamic ranges and slew rates.

I. INTRODUCTION

Magnetic techniques have been applied widely to study a variety of biological effects. Most biomagnetic applications, such as quantification of human iron storage levels in the liver and magnetocardiogram for the diagnosis of heart function [1, 2], employ the Superconducting QUantum Interference Device (SQUID) magnetometer as a sensor instrument to either map the local susceptibility variations of tissues or detect the very weak biomagnetic field (in the range of femtotesla to picotesla). For such an approach, techniques to enhance the field sensitivity of

SQUID and the accuracy of measurements are the key to this technology, and have attracted considerable efforts in research. Along with these concerns, an ideal SQUID magnetometer should also possess a wide dynamic range and a large slew rate. In the conventional SQUID readout electronics, a flux-locked loop (FLL) configuration is the most popular one being accepted. Although the slew rate increases with the modulation frequency, f_m , of the FLL, the noise bandwidth and the probability of spurious unlocking both are also increased. For a SQUID with extremely low intrinsic noise operated in an unshielded environment, the overall performance of a SQUID magnetometer for a given f_m is eventually determined by the loop sensitivity and bandwidth that have limits imposed by the impedance matching network between SQUID and the preamplifier of FLL. These issues thus call for a need to explore alternative electronic schemes [3].

A conventional FLL block diagram is shown in Fig. 1, where functions enclosed in the dashed box are implemented digitally in the present work. We have set up a Nb dc-SQUID magnetometer coupled with a second-order gradiometer. This system has been tested for its performance, and the experimental results have been compared between the analog electronics and a digital signal processor incorporated in the FLL. The loop gain, time constant, modulation flux size and frequency can be easily changed via software in the DSP method which offers flexibility not obtained in the analog scheme. In addition, DSP also allows us to implement data acquisition. Under these conditions, the flux-versus-voltage characteristics and the noise spectra of SQUID operated in FLL mode have been measured. Because the sensitivity of this magnetometer is not limited by the intrinsic noise of the SQUID sensor but by the ambient noise, a shielded cylinder with a lid has been constructed to

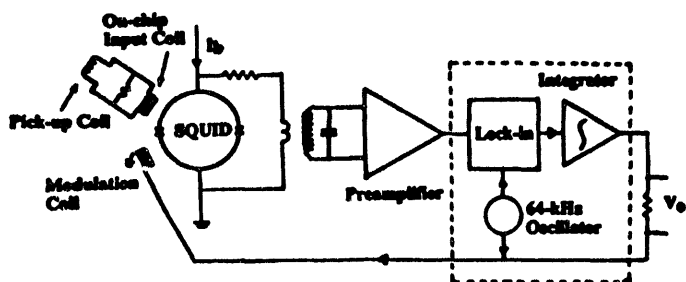


Fig. 1. A block diagram of the conventional flux-locked loop (FLL) configuration. The dashed line shows the components to be implemented digitally.

house the magnetometer to check the maximum field sensitivity.

II. EXPERIMENTAL

DC-SQUID sensors, which consist of two identical weak links (i.e., the tunnel junctions) symmetrically inserted in a superconducting ring of inductance L_S [4], and analog readout electronics are manufactured by Conductus [5]. SQUIDs are fabricated by the all-refractory Nb/Al/Al₂O₃/Nb process on 510- μ m thick silicon substrates with on-chip modulation coils and integral washer damping resistors. The SQUID inductance (L_S) is 200 pH, the critical current (I_C) is 15-25 μ A, the junction shunt resistance to prevent the nonhysteretic I-V behavior has a value of 6 Ω , and the junction capacitance is 26 fF. The readout mainly comprises a transformer-coupled low-noise preamplifier (with a gain of 10^6 in the bandwidth from 30 kHz to 1 MHz), an oscillator that generates a 0-5 V square wave of flux modulation frequency 64 kHz, and a two-pole integrator (-3 dB at 10 kHz). The readout controller can be set at either the open-loop or the FLL mode. To linearize the transfer function, $V_\Phi = (\partial V / \partial \Phi)_I$, the SQUID is operated in the FLL mode, which uses a flux driven from the output of the lock-in fed back to null the input flux [6]. The noise spectra can be measured in this mode. For the digital modulated flux-locked circuit, an 80-ns AT&T WE DSP32C floating-point DSP processor with 200-kHz dual 16-bit A/D and D/A converters is employed to drive the SQUID. The details of this DSP board, the algorithm, and the equivalent circuit components incorporated in the software are described elsewhere [3].

The SQUID is mounted in a Nb can housed in a probe, and the eight leads from the SQUID chip to readout are rf-shielded. The input contacts of the SQUID are either shorted by a piece of Nb wire for testing or connected to a balanced second-order gradiometer that is insensitive to both homogeneous fields and to uniform field gradients. When connected, a closed superconducting circuit of Nb wire is formed which has the detection coil as primary and the SQUID on-chip input coil as secondary. Although the gradiometer provides discrimination against distant noise sources in favor of nearby signals of interest, it also reduces the signal energy coupled to the SQUID. The arrangement of our complete SQUID system is shown in Fig. 2, in which the SQUID sensor and the gradiometer are maintained at 4.2 K in a bath of liquid helium kept in a superinsulated fiber-glass dewar. The bottom turn of the detection coil of the gradiometer is 12 mm away from the outer bottom surface of the dewar tail.

A dc bias current, I_b , was first adjusted and passed through the parallel connection of tunnel junctions to achieve the maximum signal-to-noise ratio (S/N) when the feedback loop was flux-locked. An ac flux of frequency at 64 kHz and amplitude of about $0.25 \Phi_0$ ($= 2.07 \times 10^{-15}$ Wb, the magnetic

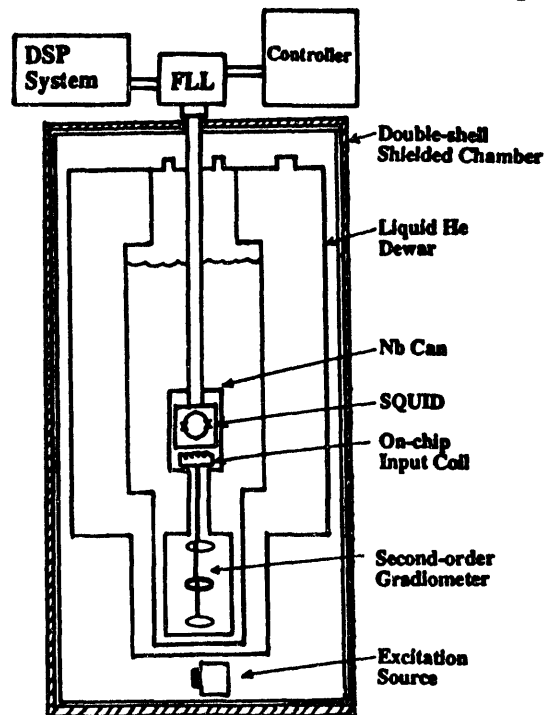


Fig. 2. The arrangement of SQUID magnetometer coupled with a second-order gradiometer.

flux quantum) was also applied to the SQUID. A two-turn coil of 6.35 mm in diameter wound from 34 AWG Cu wire to a fiber-glass rod was used to generate the desired magnetic fields. It was powered by an HP 3314A function generator, and was positioned at the dewar axis with a distance of 8.9 mm from the tail outer surface. As the Cu coil was excited, the associated magnetic field was sensed by the gradiometer to induce a current that was proportional to the instantaneous value of the applied magnetic flux (Φ_a). This current passed through the input coil and imposed a field on the SQUID. The SQUID then responded to this field, and the voltage V_S across the SQUID was recorded, which exhibited a periodic dependence on Φ_a . To reduce ambient field noise, a 39-in high shielded cylinder (with an outer dimension of 23 in) was constructed which consisted of two concentric shells, each comprising one layer of high-permeability mumetal for magnetic shielding and one aluminum (type 5086) plate for eddy-current shielding. With this cylinder, the earth's steady fields (at the latitude of about 36°) were reduced to 2 nT and 100 nT for horizontal and vertical components, respectively.

III. RESULTS AND DISCUSSION

To measure the performance of the shielded cylinder, an HP 3582A spectrum analyzer is employed to record the noise of the SQUID system in a bandwidth of 1 kHz. As compared with the noise spectrum obtained in the open environment, the dominant 60-Hz component and its harmonics have been either eliminated or significantly reduced. Because of this notable shielding property, the following measurements have been performed inside the shielded cylinder.

Figure 3 shows the response of the dc-SQUID to a 100 Hz, 10 mV peak-to-peak sinusoidal wave. As can be seen, the SQUID output voltage in the analog case is twice that in the DSP case. Because the equivalent circuit presently built in the DSP is not exactly the same as the analog FLL, this, in turn, may introduce distortion in the phase and the amplitude of the transmitted signals. Further improvement in compensating this effect is now in progress. The weakest magnetic field that can be monitored by the SQUID system has also been investigated. With a 10-kHz sampling rate and the low-frequency signal being averaged over 200 cycles, the lowest observable detected signal for

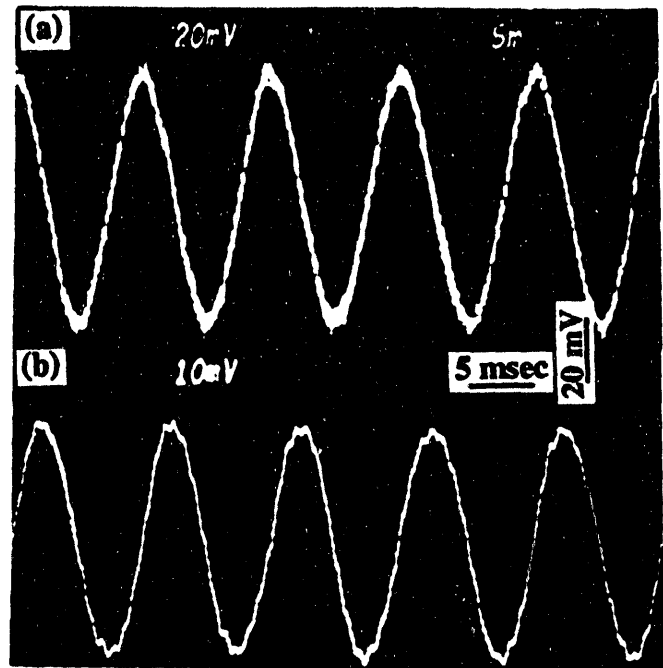


Fig. 3. SQUID responses to a 100 Hz, 10 mV peak-to-peak sinusoidal wave in (a) analog and (b) DSP FLL modes.

both analog and DSP has a peak-to-peak value of 0.2 mV. This corresponds to a field strength of 17.7 pT (see Fig. 4) sensed by the pick-up coil. However, taking into account the noise level of the system, the minimum field change that can be detected is $12.7 \text{ fT}/\sqrt{\text{Hz}}$, and the sensitivity to field is about 10.1 nT/V. In the DSP setup, due to more

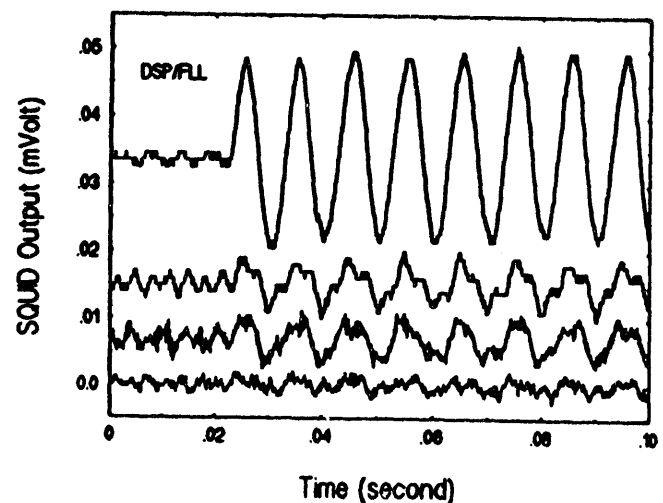


Fig. 4. The SQUID responses to various applied magnetic fields (69.2 pT, 28.3 pT, 21.1 pT, and 17.7 pT) in the DSP FLL mode.

coaxial cables being involved for communication, it is more liable to external disturbance which can cause magnetic flux popping.

By applying a small 1-Hz ac magnetic field via the two-turn Cu coil, the voltage noise density, S_V (V/ $\sqrt{\text{Hz}}$), can be measured, and the flux noise density S_Φ ($\Phi_0/\sqrt{\text{Hz}}$) can also be calculated by the expression, $S_\Phi = S_V/(\partial V/\partial \Phi)_I$. The noise characteristics of the SQUID are usually measured with the bias current near the critical current where $(\partial V/\partial \Phi)$ is at its maximum. Figure 5 shows the

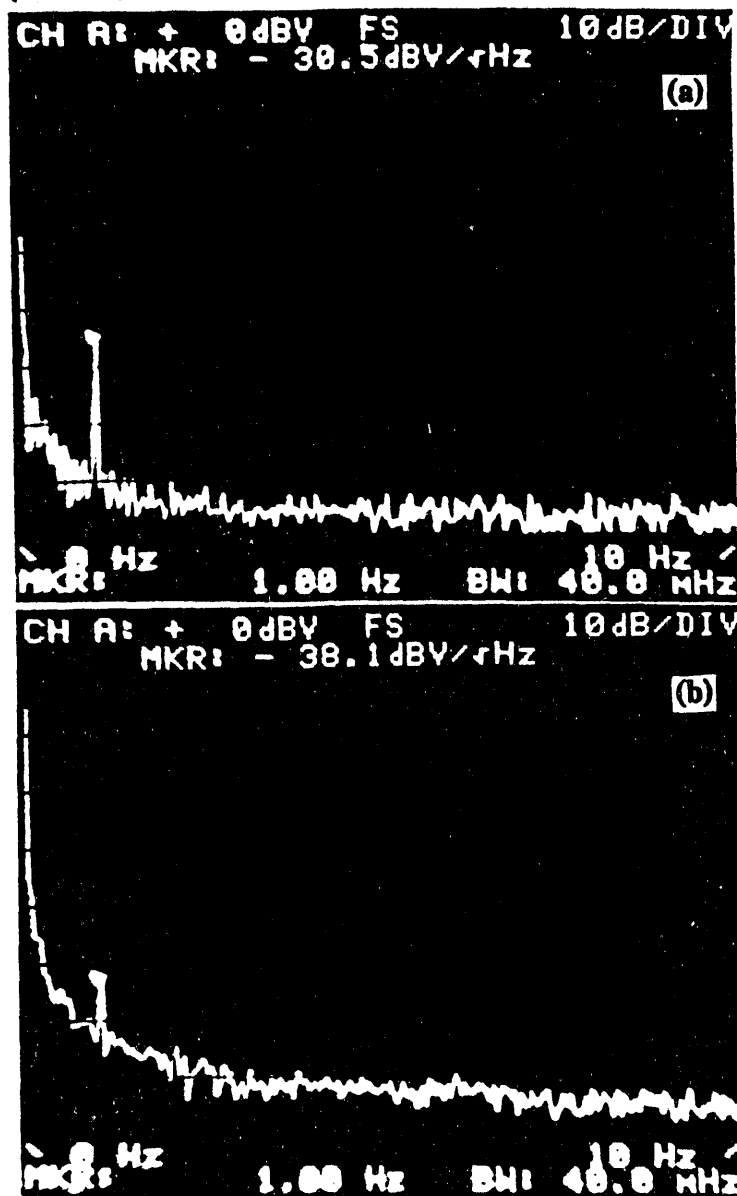


Fig. 5. Voltage noise spectrum at 4.2 K for a dc-SQUID with (a) analog and (b) DSP FLL, where x-axis: 1 Hz/div and y-axis: 10 dB/div.

voltage noise spectrum of the SQUID operated at 4.2 K in flux-locked mode by analog electronics and DSP, respectively. As can be seen, these two cases are very comparable, and at $f > 2$ Hz, S_V is in the frequency-independent white noise region, whereas below 2 Hz, $1/f$ begins to dominate over white noise. The $1/f$ noise is generally believed to originate from either critical current fluctuations [7, 8] or the motion of magnetic vortices [9]. The equivalent flux noise is $2.5 \mu\Phi_0/\sqrt{\text{H}}$ ($3.3 \mu\Phi_0/\sqrt{\text{Hz}}$) in the white noise and $4 \mu\Phi_0/\sqrt{\text{Hz}}$ ($13 \mu\Phi_0/\sqrt{\text{Hz}}$) at 1 Hz for the case of analog (DSP) FLL. If the SQUID input contacts are shorted, $1/f$ corner frequency shifts to 0.25 Hz.

The maximum ac sinusoidal field that does not cause the SQUID magnetometer system to saturate has been characterized for the analog case as illustrated in Fig. 6, from which the maximum slew rates are estimated to be 9 $\mu\text{T}/\text{sec}$ at 10 Hz and 40 $\mu\text{T}/\text{sec}$ at 100 Hz. In the DSP case, interference caused by the use of coaxial cables has to be eliminated before the same measurement is performed. This goal is now being targeted in our laboratory. For a constant applied magnetic field, the bandwidth is investigated for the SQUID driven by analog and DSP FLL modes, and the results are compared in Fig. 7. The DSP FLL seems to show a narrower bandwidth, but this does not imply a poorer system. As we mentioned earlier, we have not yet optimized the DSP scheme, and we believe that there will be further improvement. The dynamic range of the analog SQUID is in the order of 10^6 . Because the speed of A/D converters in

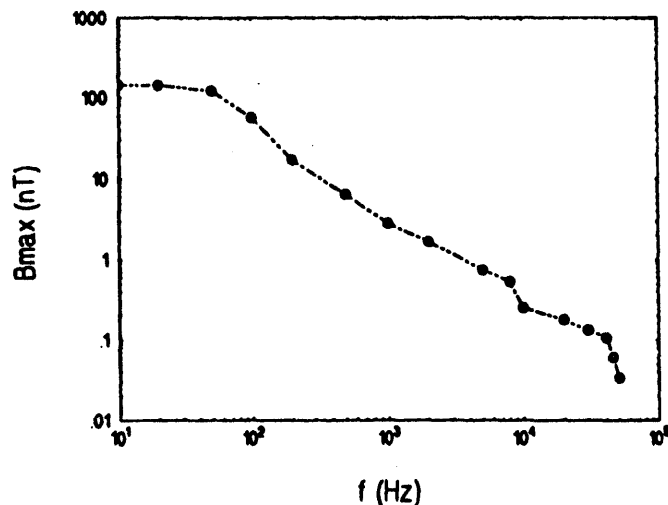


Fig. 6. Maximum magnetic field that can be fed to analog FLL without causing saturation problems.

DSP is usually the key to the dynamic range, a higher value of dynamic range in digital SQUID should be achieved if an 18-bit or higher resolution is chosen.

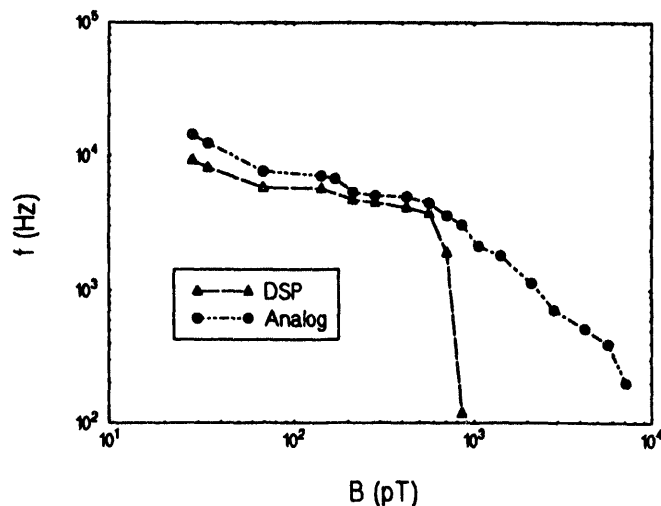


Fig. 7. A comparison of the bandwidth in the SQUID system between analog and DSP FLL modes.

IV. CONCLUSION

We have demonstrated that the conventional analog flux-locked loop modulation, integration, feedback, and detection used in dc-SQUIDs can be implemented digitally by replacing the components after the preamplifier in the analog scheme. The frequency and phase response of the digital SQUID can be adjusted without the selection of precision components which provides us with more flexibility than analog electronics. The possibility of single DSP board to drive several SQUID sensors may result in effective cost reduction. The DSP approach also allows us to implement data acquisition and adaptive noise reduction. Simulation of noise characteristics of the complete circuit with the SQUID parameters taken into account is thus now underway such that the sensitivity of digital SQUID can be enhanced. Although our current DSP-SQUID results do not show the performance better than that obtained in the analog electronics, a further improvement, such as the enhancement of S/N ratio, slew rates, and dynamic ranges, could be made if equivalent circuits and operating points both are optimized.

References

- [1] G.M. Brittenham, D.E. Farrell, J.W. Harris, E.S. Feldman, E.H. Danish, W.A. Muir, J.H. Tripp, and E.M. Bellon, *New Engl. J. Med.* **307**, 1671 (1982).
- [2] D. Cohen, E. Edelsack, and J.E. Zimmerman, *Appl. Phys. Lett.* **16**, 278 (1970).
- [3] R. R. Bracht, P.J. Kung, P.S. Lewis, and E.R. Flynn, in this proceeding.
- [4] J. Clarke, *Science* **184**, 1235 (1974).
- [5] Conductus, Inc., 969 West Maude Avenue, Sunnyvale, CA 94086.
- [6] J. Clarke, *Proc. IEEE*, vol. **61**, 8 (1973).
- [7] C.T. Rogers and R.A. Buhrman, *IEEE Trans. Mag.* **19**, 453 (1983).
- [8] M. Kawasaki, P. Chaudhari, and A. Gupta, *Phys. Rev. Lett.* **68**, 1065 (1992).
- [9] M.J. Ferrari, M. Johnson, F.C. Wellstood, J. Clarke, P.A. Rosenthal, R.H. Hammond, and M.R. Beasley, *Appl. Phys. Lett.* **53**, 695 (1988).

DATE

FILMED

10/6/94

END

